Journal of Hazardous Materials 513 (2026) 142480

Contents lists available at ScienceDirect

Journal of Hazardous Materials

journal homepage: www.elsevier.com/locate/jhazmat

Dynamic shifts and molecular regulatory mechanisms of three predominant horizontal antibiotic resistance gene transfer modes during photocatalytic disinfection

Yiwei Cai [a,b], Yongjie Liu [a,b], Guiying Li [a,b], Po Keung Wong [a,b], Taicheng An [a,b,*], Huijun Zhao [a,b]

[a] Guangdong Key Laboratory of Environmental Catalysis and Health Risk Control, Guangdong-Hong Kong-Macao Joint Laboratory for Contaminants Exposure and Health, Institute of Environmental Health and Pollution Control, Guangdong University of Technology, Guangzhou 510006, China
[b] Guangdong Basic Research Center of Excellence for Ecological Security and Green Development, Guangdong Technology Research Center for Photocatalytic Technology Integration and Equipment Engineering, School of Environmental Science and Engineering, Guangdong University of Technology, Guangzhou 510006, China

HIGHLIGHTS

- Early photocatalysis promotes conjugation via ARG-enhanced host resistance targets.
- Prolonged photocatalysis shifts HGT dominance from conjugation to transduction.
- ARG-conferred target enhancement dictates HGT pathway preference.
- Bacterial inactivation alone is insufficient for disinfection risk assessment.
- Transduction persists after disinfection as a stable ARG dissemination route.

GRAPHICAL ABSTRACT

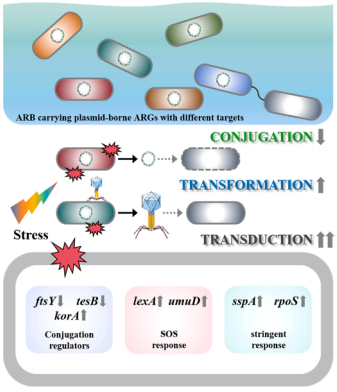

ARTICLE INFO

Keywords:
Antibiotic resistance genes
Horizontal gene transfer
Photocatalytic disinfection
Regulatory mechanisms
Transduction

ABSTRACT

The spread of antibiotic resistance genes (ARGs) through horizontal gene transfer (HGT) during disinfection processes poses a significant challenge to water safety. However, the pathway-specific dynamics and regulatory mechanisms remain insufficiently elucidated. This study employed engineered strains harboring plasmids carrying six different ARGs targeting distinct cellular processes to demonstrate photocatalytic disinfection exhibiting unique and time-resolved effects on HGT. The results demonstrate that, although conjugation initially dominated HGT (37.7% – 98.3%), prolonged photocatalytic disinfection triggered a marked shift toward transduction (70% – 92% after 40 min), revealing a critical transduction-associated residual risk. The conjugation of various ARGs was transiently and heterogeneously enhanced (1.6 – 11.6 folds) during early photocatalysis (10 – 20 min), with strains carrying protein-targeting ARG exhibiting the greatest and most sustained

* Corresponding author at: Guangdong Key Laboratory of Environmental Catalysis and Health Risk Control, Guangdong-Hong Kong-Macao Joint Laboratory for Contaminants Exposure and Health, Institute of Environmental Health and Pollution Control, Guangdong University of Technology, Guangzhou 510006, China.
E-mail address: antc99@gdut.edu.cn (T. An).

https://doi.org/10.1016/j.jhazmat.2026.142480
Received 26 February 2026; Received in revised form 25 April 2026; Accepted 19 May 2026
Available online 20 May 2026
0304-3894/© 2026 Elsevier B.V. All rights are reserved, including those for text and data mining, AI training, and similar technologies.

promotion due to their higher tolerance to photocatalytic stress. This finding elucidates the role of resistance targets in modulating conjugation during disinfection. Transformation exhibited a sustained enhancement (1.4 – 2.6 folds), whereas transduction maintained remarkably stable throughout the treatment. Mechanistically, photocatalytic disinfection elevated intracellular reactive oxygen species (ROS) levels, total antioxidant capacity, and membrane permeability. These changes synergistically regulated key functional genes, characterized by an initial up-regulation of conjugation-related genes (*ftsY*, *tesB*), followed by the sustained activation of SOS response genes (*lexA*, *umuD*) and stringent response genes (*sspA*, *rpoS*), providing a mechanistic explanation for the dynamic shifts among the three HGT modes. These findings highlight the inadequacy of relying solely on bacterial inactivation as an efficacy metric for disinfection and elucidate the differential regulation of HGT among ARGs with distinct resistance targets.

1. Introduction

The shortage of global clean water resources has long been a major environmental and public health issue [1]. As such, the reuse of reclaimed wastewater has emerged as a potential strategy to alleviate water scarcity and has garnered increasing attention. However, such reclaimed water typically contains a variety of pathogens and antibiotic-resistant bacteria (ARB) [2,3]. If it is not treated or not properly treated, it will pose a significant risk to human and animal health as well as ecosystem safety. Therefore, effective water disinfection is essential before the reuse of any form of reclaimed water [4]. However, traditional water disinfection processes often fail to completely eliminate ARB, leading to the persistence and even enrichment of bacteria carrying plasmids with multiple antibiotic resistance genes (ARGs) [5,6]. Furthermore, some emerging advanced disinfection processes (such as photocatalysis) exhibit limitations in controlling the spread of antibiotic resistance under sub-lethal conditions [7]. Therefore, restricting the dissemination of ARGs during water reuse remains a significant challenge faced by current water disinfection technologies.

Ideally, water disinfection should achieve complete inactivation of ARB and destroy the DNA structure and function of ARGs, thereby preventing the spread of antibiotic resistance entering wastewater treatment plants after water disinfection through horizontal gene transfer (HGT). However, during the water disinfection process, some ARB may survive, and the vertical transfer capacity of ARGs remains largely unaffected. ARGs may even be transferred to new bacterial hosts through HGT, leading to the emergence of novel ARB and even multidrug-resistant strains [8,9]. This phenomenon can be attributed low-dose disinfection upregulating HGT-related genes, thereby increasing the transfer frequency of ARGs. For example, ultraviolet (UV) radiation, one of the most widely used water disinfection technologies, has been shown to potentially facilitate the HGT of ARGs under improper application conditions, rather than ensuring their rapid elimination [10]. This is primarily attributed to its limited effectiveness in disrupting the structural integrity and biological activity of ARGs [11,12]. In addition, other traditional water disinfection methods such as chlorination and ozonation have also been proven to facilitate the HGT of ARGs [13,14]. Under low-dose or sub-lethal disinfection conditions, the occurrence of HGT in treated water may be further accelerated, a phenomenon often described as an effect within the framework of the "hormesis concept" [15]. An increasing body of evidence indicates that insufficient water disinfection will fail to achieve complete elimination of ARGs, but rather promotes the spread of antibiotic resistance through various HGT pathways, including conjugation, transformation, and transduction. For example, chlorination has been proven to promote the transfer of plasmid-mediated ARGs between different genera through natural transformation, thereby facilitating the emergence of novel ARB [16]. Unfortunately, as an emerging advanced oxidation process, photocatalysis has also been found to promote the transduction of ARGs during water disinfection [17]. In addition, sub-lethal doses of UV or photocatalytic disinfection can enhance the conjugative transfer of multiple ARGs to some extent [7,10]. Previous researches have clarified that various minerals present in the environment are prone to generating photocatalytic disinfection effects under natural light exposure [18,19]. However, the specific contributions of different HGT pathways and their regulatory mechanisms during photocatalytic water disinfection remain to be elucidated. Furthermore, since different disinfection technologies exert their effects through distinct inactivation mechanisms and exhibit varying efficacies against different ARG targets, the preferential activation of specific HGT pathways may be governed by target-dependent regulatory processes.

Herein, a systematic comparison of three major HGT modes (e.g. conjugation, transformation, and transduction) was conducted under sub-lethal photocatalytic disinfection conditions, aiming to quantitatively evaluate the contribution of each HGT pathway to the spread of ARGs and their potential mechanisms. To further evaluate bacterial tolerance to photocatalytic disinfection, six *Escherichia coli* strains carrying different plasmid harboring specific ARG (*mcr-1*, $bla_{CTX\text{-}M}$, *tetM*, *sul3*, *gyrA96*, or *rpoB331*) were constructed. These ARGs represent resistance to antibiotics targeting different cellular processes, including cell membrane, cell wall, protein synthesis, folate metabolism, DNA replication, and RNA transcription. In addition, experimental systems for three HGT modes were established to quantify the transfer potential and relative proportions of ARGs with different resistance targets. Meanwhile, the expression levels of ARGs, target-specific resistance-related genes, and HGT-related genes were analyzed to further clarify the specific contributions and regulatory mechanisms of different ARG transfer pathways. These research findings provide deeper insights into the roles and regulatory mechanisms of different HGT modes in the spread of ARGs with distinct resistance targets, offering new strategic guidance for controlling the transmission of antibiotic resistance during water disinfection processes.

2. Materials and methods

2.1. Culture of antibiotic-resistant bacteria and P1 phage

E. coli DH5α strains resistant to polymyxin B (PB), tetracycline (TET), cefotaxime (CTX), rifampicin (RA), nalidixic acid (NAL), and sulfamethoxazole (SMZ) (denoted as *E. coli* DH5α (PB), *E. coli* DH5α (TET), *E. coli* DH5α (CTX), *E. coli* DH5α (RA), *E. coli* DH5α (NAL), and *E. coli* DH5α (SMZ), respectively) were constructed as model ARB with distinct antibiotic resistance targets. The construction procedures for these strains are provided in Text S1. Each strain was cultured in Luria-Bertani broth (Sangon, China) supplemented with the corresponding antibiotics at a concentration determined by its minimum inhibitory concentration (MIC). Cultures were incubated overnight at 37 °C with shaking at 180 rpm and subsequently used for HGT and mechanistic analysis. Detailed characteristics of the ARB strains and the concentrations of antibiotics used are summarized in Table S1. The selected ARGs collectively cover the major antibiotic mechanisms of action. Notably, the target antibiotics include PB, considered a last-line defense agent; CTX, a widely used β-lactam antibiotic; TET, a representative tetracycline-class drug; as well as SMZ and RA, which are common representatives of sulfonamide and rifamycin antibiotics, respectively. The P1 phage (GENMEND SCIENTIFICS INC, USA) was propagated by lysing *E. coli* DH5α (Sangon, China). Prior to transduction experiments, the transducing activity of the P1 phage was preliminarily verified

through plaque formation assays on solid medium containing the corresponding antibiotic, with specific methods as described in Text S1.

2.2. Photocatalytic water disinfection

The photocatalytic water disinfection experiments were conducted using a multi-channel photochemical reaction system (Perfectlight, China). A TiO_2 nanotube array fabricated on titanium foil was employed as the photocatalyst and irradiated to UV light (365 nm, 150 mW·cm^{-2}) in the presence of ARB. Preliminary testing determined that exposure duration was be set at either 40 min or 24 h. Detailed experimental procedure followed the previously established methods [19] as described in Text S2. Before photocatalytic disinfection, by filtering to remove extracellular plasmids and eliminate interference with the transformation experiment.

2.3. Horizontal gene transfer experiments

The three main modes of HGT (conjugation, transformation, and transduction) were investigated to evaluate the impact of photocatalytic water disinfection on the spread of ARGs. Before mating, free extracellular plasmids in the bacterial culture were removed by filtration to prevent transformation from occurring during conjugation experiments. Free DNA in the bacterial culture was obtained through filtration, and its transformation efficiency was measured. The transfer efficiency of phage P1 to ARB was determined to establish the optimal phage concentration (Figs. S1 and S2) prior to evaluating the impact of photocatalytic disinfection on the transduction of ARG. In the HGT experiments, the initial concentration of all donor and recipient *E. coli* was 10^8 CFU mL^{-1}. Detailed methods for measuring HGT of ARGs targeting different resistance mechanisms are provided in Text S3.

2.4. Gene expression assay

To confirm that ARGs retain the ability to undergo HGT following photocatalytic water disinfection, quantitative polymerase chain reaction (qPCR) was performed. In addition, qPCR was used to analyze the expression levels of relevant genes in donor bacteria to further clarify the impact of photocatalytic water disinfection on HGT mechanisms in ARB with different resistance targets. Following protocol validation and optimization, qPCR was carried out on a CFX 96 Touch thermal cycler (Bio-Rad, USA) using SYBR Green qPCR Mix (Monad, China). Each 20 μL reaction mixture contained 10 μL of SYBR Green qPCR Mix, 0.75 μL each of forward and reverse primers (10 μM), 2 μL of DNA template, and 6.5 μL of nuclease-free water. The thermal cycling conditions and calculation method for ARG quantification were based on a previously reported study [20]. The 16S rRNA gene served as the internal control. Primer sequences are provided in Table S2, and the full experimental protocol is detailed in Text S4. All qPCR assays were performed with at least three technical replicates. Detailed description of the qPCR analysis, including primer sequences for target ARGs and standard curve data, is provided in Text S5. As shown in Table S3, the expression of 16S rRNA remained stable relative to total RNA during the first 40 min of photocatalysis. Therefore, the normalization effectiveness of 16S rRNA as an internal control was not compromised.

The analyzed genes included ARGs (bla_{CTX-M}, *mcr-1*, *tetM*, *sul3*, *gyrA96*, *rpoB331*), penicillin-binding proteins (*PBP2*, *PBP5*), outer membrane porins (*ompA*, *ompF*), protein synthesis regulators (*rsmB*, *rsmE*), dihydrofolate synthesis genes (*folA*, *folP*), DNA gyrase A (*gyrA*), RNA polymerase β-subunit (*rpoB*), conjugation-related genes (*ftsY*, *tesB*, *korA*), transformation-related genes (*umuD*, *lexA*), and transduction-related genes (*sspA*, *rpoS*).

2.5. Statistical analysis

All experiments were conducted independently and repeated at least three replicates. Data are displayed as mean ± standard deviation. Statistical significance ($p < 0.05$) was established using one-way analysis of variance (ANOVA).

3. Results and discussion

3.1. Conjugation dominance and gene-specific inactivation kinetics of ARGs

Prior to photocatalytic bacterial inactivation, the baseline characteristics of HGT for six different ARGs targeting distinct resistance were systematically evaluated. The results clearly indicated that conjugation is the primary mode of ARG dissemination under non-treated conditions. As shown in Fig. 1a–c, the densities of transconjugants, transformants, and transductants differed significantly across various ARGs. Notably, ARGs conferring resistance to CTX (bla_{CTX-M}), SMZ (*sul3*) and TET (*tetM*) displayed the highest transconjugant densities, exceeding those of other ARGs (Fig. 1a). By comparison, the absolute efficiency of transformation (Fig. 1b) and transduction (Fig. 1c) were typically 1 – 2 orders of magnitude lower than that of conjugation. This suggests that plasmid-mediated conjugation should be prioritized as the primary process in the initial environmental risk assessment of ARGs. Additional analysis of the relative contributions of the three HGT modes (Fig. 1d) strongly supported this conclusion. Conjugation was accounted for 37.7% – 98.3% of all detected HGT events and the primary mechanism for the spread of ARG. Transformation and transduction contributed 0.3% – 5.6% and 1.4% – 56.7%, respectively, indicating that free DNA-mediated and phage-mediated gene flow play relatively minor roles before photocatalytic bacterial inactivation. Notably, the distribution of preferred modes also varied among different ARGs. Genes resistance to CTX, TET, SMZ, and RA (bla_{CTX-M}, *tetM*, *sul3* and *rpoB331*) were primarily disseminated via conjugation (accounting for 88.7%, 98.3%, 95.2%, and 83.7%), whereas a substantial proportion of Genes resistance to PB (*mcr-1*, 56.7%) and NAL (*gyrA96*, 54.9%) were transferred via transduction. It suggests that plasmids carrying these genes may be more likely to undergo HGT between different bacteria via the pathway of phage-mediated transduction.

In sum, these results clearly outlined the risk characteristics of ARG spread prior to photocatalytic disinfection, establishing conjugation as the most efficient and widespread transmission mechanism. This finding aligns with the widespread consensus in the field of environmental microbiology that conjugation mediated by mobile genetic elements such as plasmids is the main driving factor for the rapid spread of ARGs among various bacterial populations in both engineered and natural environments [21,22]. Moreover, the significant role of transduction in spreading PB and NAL resistance genes highlights that certain ARGs may be more predisposed to antibiotic resistance spread via phages [23]. This finding underscores the urgent need to develop water disinfection technologies capable of effectively disrupting cell-to-cell contact and plasmid transfer, while also establishing a critical benchmark for evaluating the differential inhibitory effects of photocatalytic disinfection on various HGT pathways.

The efficacy and kinetics of photocatalytic inactivation were systematically evaluated for host bacteria carrying different of ARGs. The results indicate that although photocatalytic disinfection can achieve broad-spectrum inactivation of all conjugated *E. coli* strains, the bacterial inactivation kinetics vary significantly depending on the specific ARG carried, highlighting its importance as a key determinant in subsequent risk assessment of HGT. As shown in Fig. S3, photocatalytic water disinfection caused a rapid and significant decrease in cell viability across all strains, including the susceptible host strain and those harboring six distinct ARGs. Within 50 min, the densities of all strains decreased by more than 8 logs, confirming that the photocatalytic process exhibits strong and broad-spectrum bactericidal activity regardless of the presence of specific resistance-determining factors. However, a more detailed observation of bacterial inactive dynamics revealed

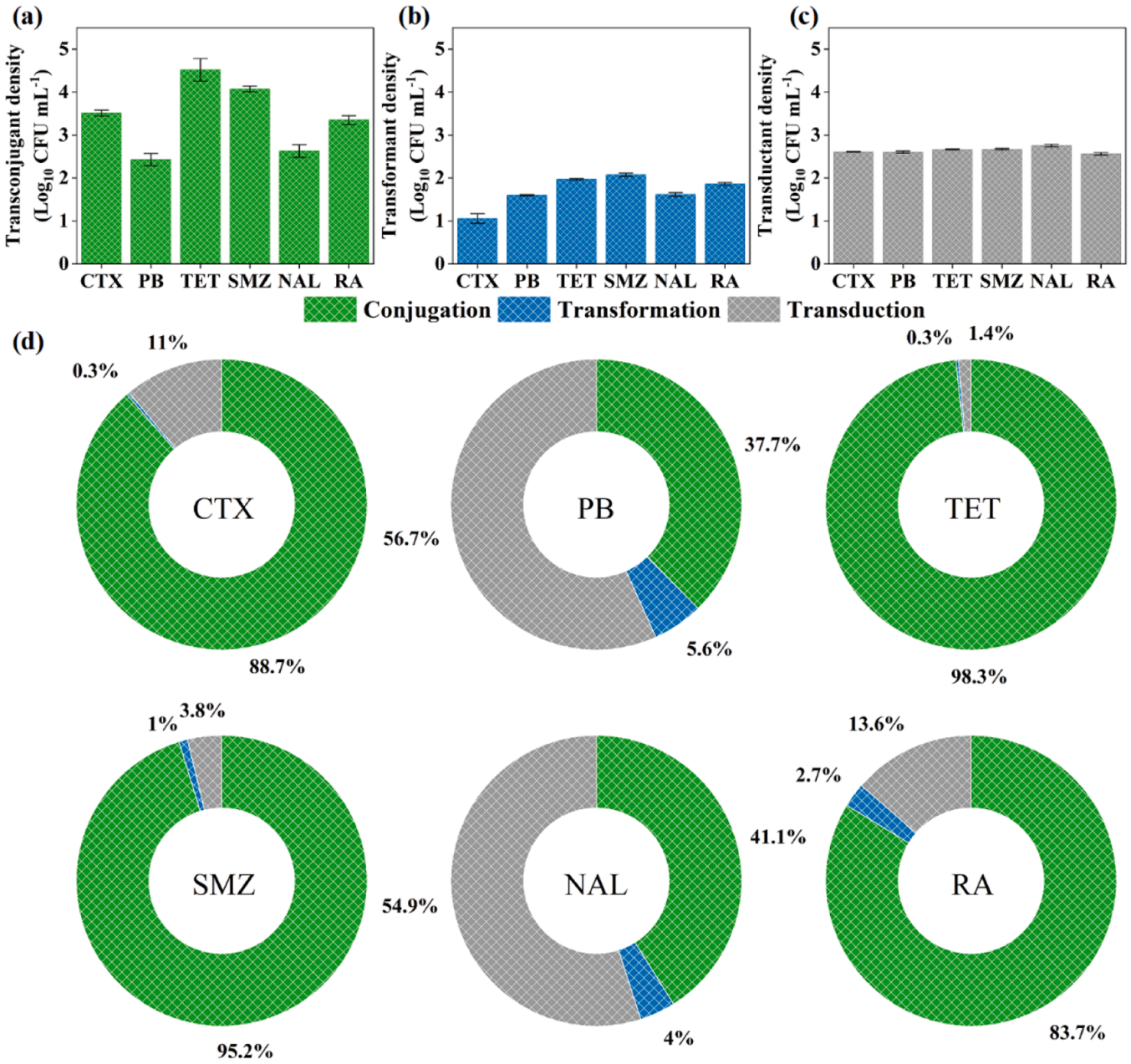

Fig. 1. Horizontal gene transfer of antibiotic resistance genes across different resistance targets prior to photocatalytic water disinfection: (a) conjugation, (b) transformation, and (c) transduction frequencies, and (d) their relative contribution proportion. CTX: cefotaxime resistance gene (bla_{CTX-M}); PB: polymyxin B resistance gene (*mcr-1*); TET: tetracycline resistance gene (*tetM*); SMZ: sulfamethoxazole resistance gene (*sul3*); NAL: nalidixic acid resistance gene (*gyrA96*); RA: rifampicin resistance gene (*rpoB331*).

significant differences between strains carrying different ARGs (Fig. S3). In detail, strains carrying the genes resistance to CTX, PB and TET (bla_{CTX-M}, *mcr-1* and *tetM*) exhibited persistence during the initial inactivation phase (10 – 20 min), with their viable bacterial density decreasing at a significant slower rate compared to the susceptible *E. coli* DH5α strain and other strains carrying other ARGs. Based on the slope of photocatalytic bacterial inactivation kinetics (Fig. S3), the order of tolerance to photocatalysis for different strains could be summarized as *E. coli* DH5α (TET) > *E. coli* DH5α (SMZ) > *E. coli* DH5α (PB) > *E. coli* DH5α (CTX) > *E. coli* DH5α (NAL) > *E. coli* DH5α (RA) > *E. coli* DH5α. This temporary tolerance can be attributed to non-specific cross-tolerance provided by certain resistance mechanisms (such as membrane permeability barriers or efflux pump systems), which can resist the action of photogenerated reactive oxygen species (ROS) [24]. To quantitatively compare the inactivation efficiency of different ARGs, their real-time inactivation profiles during the 24 h photocatalytic inactivation process were also analyzed (Fig. 2). Obvious differences in inactivation kinetics were observed, leading to the classification of six ARGs into two distinct categories. Genes resistance to CTX, PB and NAL (bla_{CTX-M}, *mcr-1* and *gyrA96*) exhibited "slow and persistent" kinetics with lower inactivation rates (Fig. 2a, b, e). In contrast, genes resistance to TET, SMZ and RA (*tetM*, *sul3* and *rpoB331*) showed "rapid and responsive" inactivation, marked by a steep decline (approximately 2 – 3 logs) during the initial treatment phase (0 – 6 h), with levels remaining minimal throughout the experiment (Fig. 2c, d, f). The observed differences in inactivation kinetics suggest varying susceptibility to photocatalytic stress, which may be attributable to the distinct structural or functional modifications conferred by different ARGs on their respective

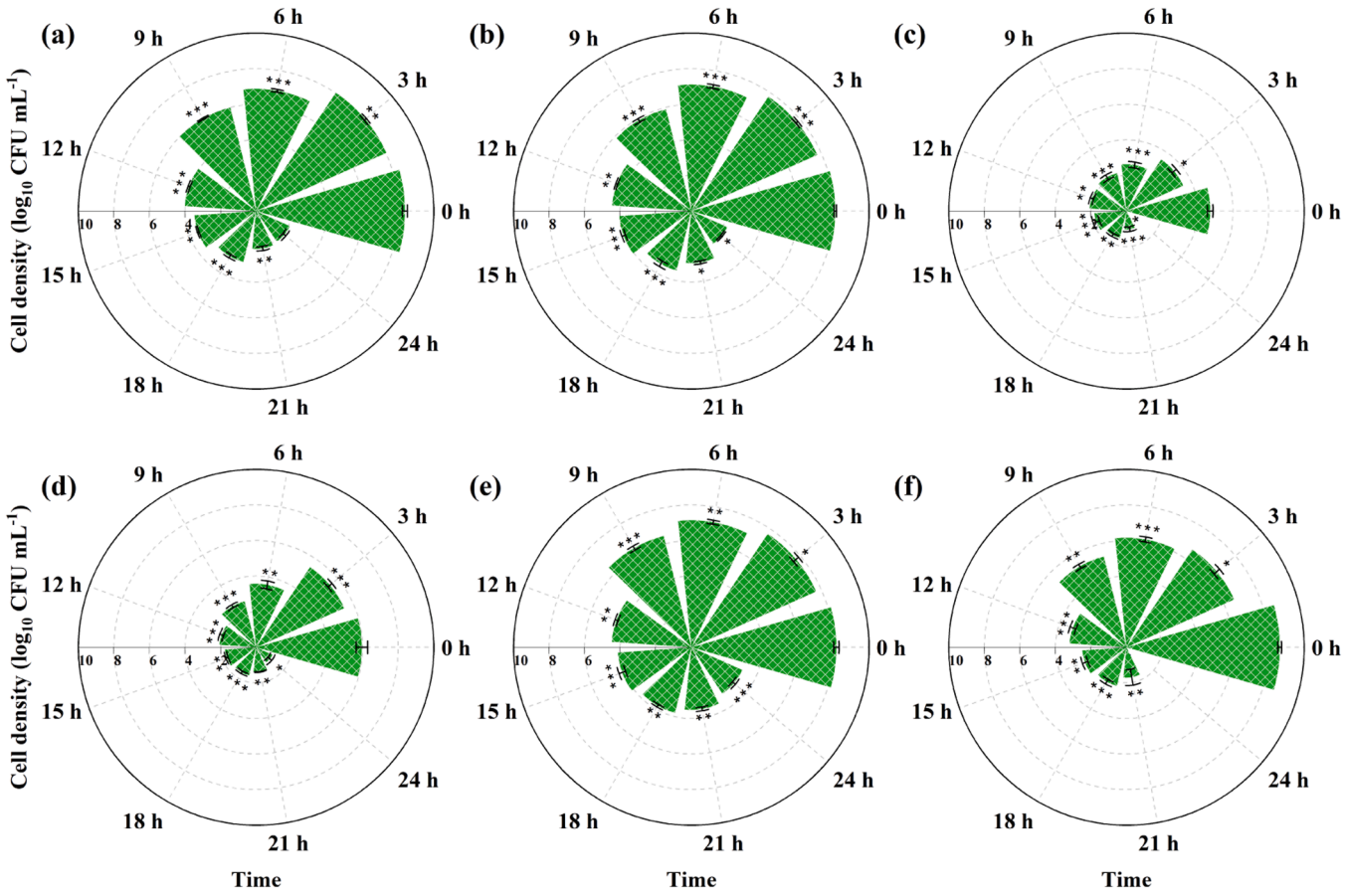

Fig. 2. Photocatalytic inactivation efficiencies of antibiotic resistance genes with different resistance targets: (a) cefotaxime (CTX) resistance gene ($bla_{CTX\text{-}M}$); (b) polymyxin B (PB) resistance gene (*mcr-1*); (c) tetracycline (TET) resistance gene (*tetM*); (d) sulfamethoxazole (SMZ) resistance gene (*sul3*); (e) nalidixic acid (NAL) resistance gene (*gyrA96*); (f) rifampicin (RA) resistance gene (*rpoB331*). Significant differences were tested with one-way ANOVA analysis, *: $0.01 < p \leq 0.05$, **: $0.001 < p \leq 0.01$, ***: $p \leq 0.001$.

host bacteria [25,26]. The difference in inactivation kinetics is crucial because it suggests that bacterial populations carrying distinct ARGs will be selectively enriched or eliminated under photocatalytic stress. Strains carrying genes resistance to CTX, PB and NAL, due to their enhanced survival capabilities, have a longer timeframe to spread resistance through conjugation or other HGT mechanisms, thus presenting a potentially greater environmental risk.

In summary, while photocatalysis can effectively inactivate broad-spectrum ARB, its efficiency is significantly influenced by the specific type of ARG present. Identifying and understanding the differences in ARGs is crucial for accurately evaluating and optimizing strategies aimed at controlling the spread of antibiotic resistance. The persistence of certain ARGs underscores their potential as persistent contaminants and highlights the issue of their higher subsequent risk of HGT.

3.2. Dynamic changes of HGT and risk reevaluation of different ARGs

To investigate the dynamic changes of three predominant horizontal antibiotic resistance gene transfer modes during photocatalytic disinfection, the density changes of products from three HGT pathways were systematically monitored throughout the entire inactivation process. The findings showed substantial variations in the effectiveness of photocatalytic disinfection across different HGT pathways. Inactivation kinetics demonstrated that photocatalysis completely eliminated the cultivability of all ARB within 50 min (Fig. S3a). In contrast, the TiO_2 nanotube array system without UV irradiation exhibited no bactericidal effect (Fig. S3b), confirming that the TiO_2 nanotube arrays themselves are non-toxic to the tested ARB. Accordingly, this study focuses on the dynamic shifts in HGT modes during the initial 40 min of photocatalytic treatment. A notable resurgence in conjugation and transformation frequencies was observed during the process, underscoring a potential risk that may be overlooked in standard disinfection evaluations. The detailed analysis of the conjugation pathway showed that photocatalytic disinfection significantly enhanced conjugative transfer for most ARGs at the initial stage (10 – 20 min) (Figs. 3a and S4a). The conjugation frequency of genes resistance to CTX, PB, SMZ, and NAL ($bla_{CTX\text{-}M}$, *mcr-1*, *sul3* and *gyrA96*) reached their peak at 10 min, increasing to approximately 1.6-, 11.6-, 5.4-, and 2.5-fold, respectively. A similar promotional effect was observed for TET resistance gene (*tetM*). Its conjugation frequencies peaked at 20 min, increasing by 9.6-fold (Fig. 3a), followed by inhibition. Although the cell density of all ARB decreased significantly within the initial 10 – 20 min of photocatalytic disinfection, the conjugation frequency is defined as the ratio of trans-conjugant colonies on double-antibiotic plates to recipient cells on single-antibiotic plates. Consequently, the observed enhancement of conjugation during this early period represents an absolute promotion (a genuine increase in total transfer events). Furthermore, the loss of bacterial viability during the initial 10 – 20 min reflects only a partial loss of culturability, as the plasmids carried by the remaining culturable bacteria retained their conjugative function. To substantiate this, we performed live/dead staining, confirming that the majority of bacteria retained their viability (Fig. S5). Notably, the loss of cultivability does not equate to the loss of conjugative function—a distinction that has not been demonstrated in any previous publication. Bacteria that have lost cultivability may merely enter a viable but non-culturable dormant state. Whether such dormant bacteria are capable of undergoing

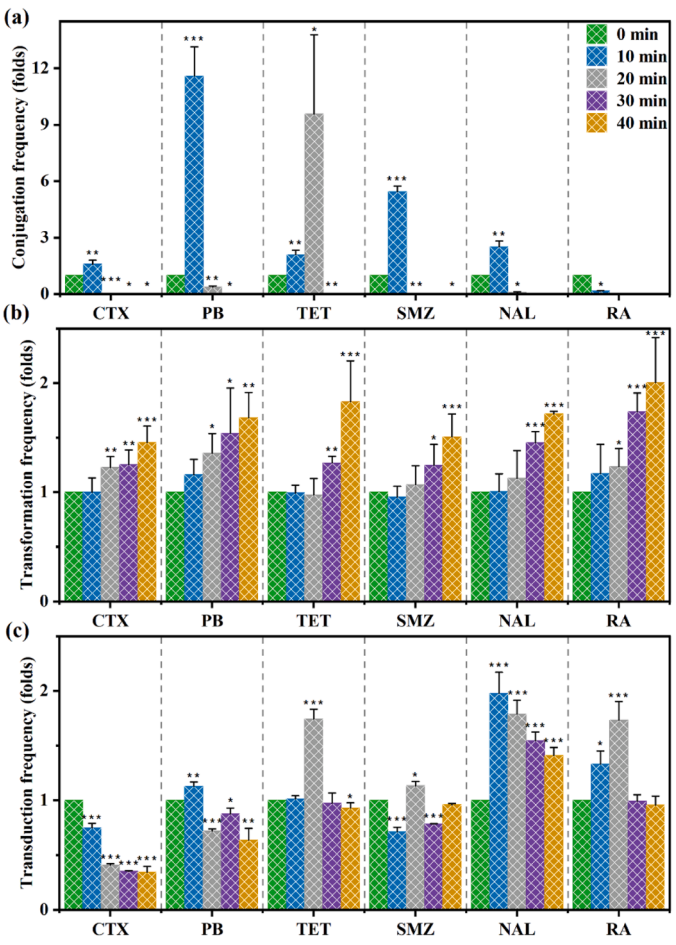

Fig. 3. Temporal changes in (a) conjugation, (b) transformation, and (c) transduction frequencies of different antibiotic resistance genes. CTX: cefotaxime resistance gene ($bla_{CTX\text{-}M}$); PB: polymyxin B resistance gene (*mcr-1*); TET: tetracycline resistance gene (*tetM*); SMZ: sulfamethoxazole resistance gene (*sul3*); NAL: nalidixic acid resistance gene (*gyrA96*); RA: rifampicin resistance gene (*rpoB331*). Significant differences were tested with one-way ANOVA analysis, *: $0.01 < p \leq 0.05$, **: $0.001 < p \leq 0.01$, ***: $p \leq 0.001$.

conjugation or other HGT events represents an important direction for future research. Transconjugant density fell below the detection limit after 40 min treatment (Fig. S4a). The significant change of conjugation frequency is consistent with the "hormesis concept" [15], which posits that low-dose or short-term photocatalytic exposure can promote the conjugation of ARGs. The underlying mechanism likely involves a disruption of the balance between oxidative stress levels and antioxidant capacity. At the early stage of photocatalytic treatment, all ARB exhibited changes in oxidative stress levels (Fig. S6a). Specifically, *E. coli* DH5α (CTX), *E. coli* DH5α (PB), *E. coli* DH5α (NAL), and *E. coli* DH5α (RA) displayed an initial increase in intracellular ROS followed by a subsequent plateau, whereas *E. coli* DH5α (TET) and *E. coli* DH5α (SMZ) showed a sustained increase throughout the 40 min treatment (Fig. S6a). These differences are likely attributable to their respective antibiotic resistance mechanisms, as the presence of ARGs reinforces specific bacterial structures, thereby conferring differential tolerance to photocatalytic stress (Fig. S3a). Intracellular ROS generated by photocatalysis preferentially attack the more vulnerable internal targets, such as DNA and RNA, which are highly susceptible to oxidative damage. Subsequently, the external barriers (e.g. the cell wall and cell membrane) are further compromised. Consequently, *E. coli* DH5α (CTX), *E. coli* DH5α (PB), *E. coli* DH5α (NAL), and *E. coli* DH5α (RA) exhibited an earlier turning point in ROS levels. These changes in ROS levels further led to alterations in total antioxidant capacity (Fig. S6b) and membrane permeability (Fig. S7). At 10 min of photocatalytic treatment, the total antioxidant capacity of nearly all ARB was sufficient to cope with the modestly elevated ROS levels. Moreover, this mild increase in ROS may further trigger the SOS response, thereby accelerating the conjugative transfer process. Membrane permeability also exhibited a slight increase, further facilitating conjugative transfer. The only exception was *E. coli* DH5α (RA), which was the most susceptible to photocatalytic stress among all tested strains. At 20 min of treatment, only the strain with a protein-targeting ARG (*E. coli* DH5α (TET)) retained sufficient antioxidant capacity to counteract the modestly elevated ROS levels, owing to the greater tolerance conferred by its resistance target. In contrast, the other ARB experienced ROS levels that overwhelmed their antioxidant capacity, and their membrane integrity was further compromised, thereby hindering the conjugation process. Collectively, these results demonstrate that ARGs render the structural integrity of different resistance targets heterogeneous, which directly influences the conjugative transfer process. The correspondence between conjugation frequency and transconjugant density confirms this enhanced biological relevance (Fig. S4a), demonstrating that long-term or high-intensity photocatalytic disinfection is highly effective in blocking intercellular contact and plasmid transfer.

In comparison, the transformation pathway displayed more complex, gene-dependent dynamic changes (Fig. 3b). The transformation frequency of all ARGs increased gradually, reaching 1.5 – 2.0 folds of enhancement at 40 min. This enhanced mode was further supported by the transformant density in Fig. S4b, showing that all ARGs exhibited a relatively consistent increase in transformant densities over the 40 min period, even under photocatalytic stress. This modest enhancement likely results from oxidative damage to a subset of bacteria (Fig. S6), leading to the further release of intracellular ARGs into the extracellular environment. This interpretation is supported by the observed changes in membrane permeability (Fig. S7). However, this enhanced pattern was relatively weak, and 40 min of processing may not be sufficient to significantly affect the transformation of ARGs. Therefore, the transformation frequency of ARGs during 24 h photocatalytic disinfection process was further calculated (Fig. S8). The temporal changes in transformant densities exhibited distinct kinetic patterns across different ARGs. As shown in Fig. S8a, the transformant densities of all ARGs showed a significant rebound during the early treatment period (1 – 3 h). These densities increased by approximately 0.1 – 0.4 log from their initial values. The transformation frequency of all ARGs reached its peak at 1 h, increasing by approximately 1.4 – 2.6 folds (Fig. S8b), followed by gene-specific inhibition. In detail, genes resistance to TET and RA (*tetM* and *rpoB331*) transformants exhibited significant persistence, with their density remaining at approximately 10 CFU mL^{-1} even after 6 h of treatment. This persistence can be attributed to their respective resistance mechanisms and differential tolerance to photocatalytic stress. Specifically, *E. coli* DH5α (TET), owing to its protein-targeting resistance mechanism that confers the strongest tolerance to photocatalytic stress, maintained its intracellular ARGs well-protected during the initial treatment phase, leading to a slow and sustained release into the extracellular environment over time. In contrast, *E. coli* DH5α (RA) likely released a larger quantity of extracellular ARGs at the early stage of disruption, thereby contributing to a more prolonged transformation process. Similarly, CTX resistance gene ($bla_{CTX\text{-}M}$) transformants maintained a consistent presence throughout the experimental period, although its density was slightly lower than that of genes resistance to TET and RA. In comparison, transformants harboring genes resistance to PB, SMZ, and NAL (*mcr-1*, *sul3* and *gyrA96*) were significantly reduced after 3 h exposure, and their density decreased below the detection limit within 6 – 12 h. Collectively, the presence of ARGs reinforces the structural integrity of their respective resistance targets, leading to differential tolerance of the six bacterial strains to photocatalytic disinfection. Photocatalytic treatment induces intracellular ROS generation, which sequentially attacks distinct intracellular targets. Notably, *E. coli* DH5α (TET), owing to its protein-targeting resistance mechanism,

exhibits the highest tolerance to photocatalytic stress. In contrast, *E. coli* DH5α (RA) releases a substantial quantity of ARGs during the early stage of photocatalytic disruption, accounting for its persistent transformation behavior. Collectively, the observed differences in transformation frequency originate from the distinct resistance mechanisms conferred by different ARGs. Therefore, in the context of actual wastewater disinfection, in addition to monitoring the inactivation of ARB, careful consideration should also be given to the types of extracellular ARGs released, their underlying resistance mechanisms, and their transformation efficiencies.

In contrast, the transduction frequency and transductant density of all ARGs remained essentially unchanged throughout the entire photocatalytic disinfection process (Figs. 3c and S4c). This indicates that phage-mediated gene transfer is highly resistant to photocatalysis. This resistance highlights the role of phages as stable environmental vectors for the dissemination of ARGs. During photocatalytic disinfection, a systematic analysis was further conducted on the dynamic changes in the frequencies of three HGT pathways of six ARGs (Fig. 4). Conjugation was rapidly initiated after 10 min photocatalysis, driving the HGT of genes resistance to CTX, PB, TET, SMZ, and NAL ($bla_{CTX\text{-}M}$, *mcr-1*, *tetM*, *sul3* and *gyrA96*) (Fig. 4a-e). These transfers accounted for 95%, 89%, 99%, 99%, and 51% of total transfer events, respectively. Among them, $bla_{CTX\text{-}M}$, *tetM*, and *sul3* displayed a strong preference for conjugative transfer (Fig. 4a, c and d). The conjugation frequency of $bla_{CTX\text{-}M}$ reached 95% at 10 min, while transformation and transduction remained below 10%. Similarly, *tetM* and *sul3* exhibited nearly complete conjugation dependence (99%) at the 10-min mark. At this point, the bacterial stress responses (up-regulation of ROS levels) are triggered (Fig. S6a), which reduce the occurrence of transduction. Some previous studies also reported that mild stress inhibits bacterial transduction [27], but this phenomenon is reversed in further photocatalytic disinfection. With prolonging photocatalytic inactivation, the transduction of ARGs gradually dominated HGT, while the transformation played a secondary role and the conjugation almost disappeared eventually. Following 40 min photocatalysis, transduction became the predominant pathway for all ARGs, with proportions rising to 70% – 92%, while transformation accounted for the remainder (8% – 29%). This shift is attributed to the disruption of bacterial integrity induced by prolonged photocatalytic treatment [28]. The initial generation of extracellular ROS increases membrane permeability, facilitating phage infection and transduction [17,29]. Subsequent intracellular ROS production and further cellular damage concurrently inhibit conjugation [30–32], thereby promoting transduction as the dominant dissemination route of bacterial antibiotic resistance. In addition, the inactivation of bacteria merely indicates that they have completely lost culturability, while the intracellular enzymes, energy, and ARGs are still sufficient to support phage-mediated plasmid packaging. This indicates that during the photocatalytic inactivation of ARB hosts, phages, as stable gene vectors, may continuously disseminate ARGs to residual or newly invading sensitive bacteria.

Notably, this study was conducted using a well-controlled laboratory

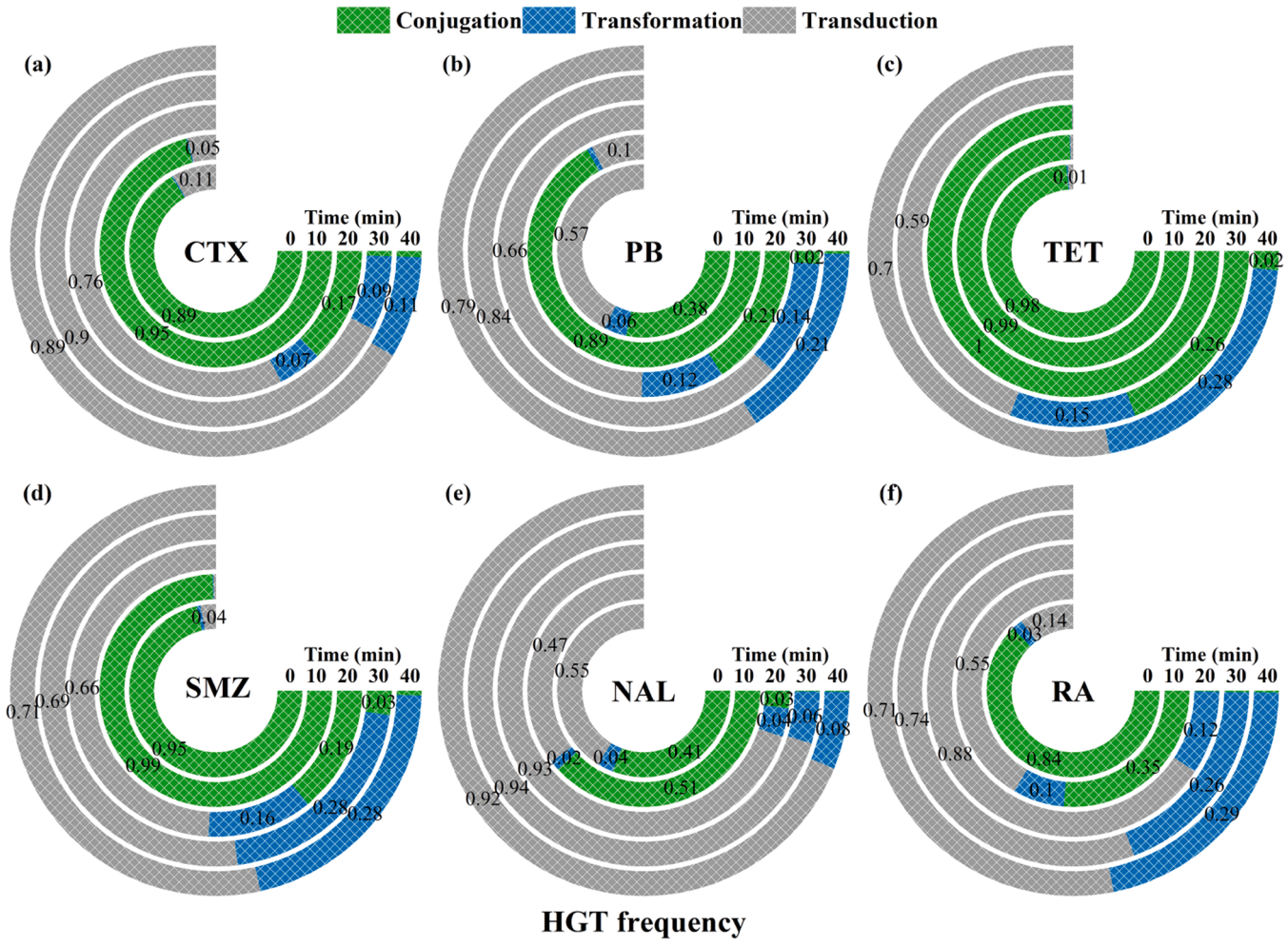

Fig. 4. Relative contribution of three horizontal gene transfer pathways of antibiotic resistance genes across different resistance targets under photocatalytic disinfection conditions: (a) cefotaxime (CTX) resistance gene ($bla_{CTX\text{-}M}$); (b) polymyxin B (PB) resistance gene (*mcr-1*); (c) tetracycline (TET) resistance gene (*tetM*); (d) sulfamethoxazole (SMZ) resistance gene (*sul3*); (e) nalidixic acid (NAL) resistance gene (*gyrA96*); (f) rifampicin (RA) resistance gene (*rpoB331*).

system employing a TiO_2 nanotube array as the photocatalyst and UV light at 365 nm as the irradiation source to investigate contributions and dynamic evolution of three major HGT pathways during photocatalytic disinfection. To specifically elucidate how different ARGs, by virtue of their distinct resistance properties and mechanisms, influence the relative contributions of HGT pathways, we constructed ARB by introducing plasmids carrying different ARGs into the same bacterial strain. This approach effectively eliminates potential confounding effects arising from intrinsic species differences. However, it is challenging to identify bacterial strains of the same species harboring plasmids with different ARGs in real wastewater or reclaimed water. Consequently, our conclusions were not further validated in authentic water matrices. Moreover, factors such as natural organic matter, ionic strength, and suspended particles in real water may influence photocatalytic efficiency, ROS generation, and the HGT processes. Nevertheless, several previous studies have indirectly corroborated the key findings of this investigation. For instance, Yu *et al.* demonstrate that TiO_2 nanotube-based UV photocatalytic disinfection for 3 h compromises bacterial integrity via ROS damage in wastewater sludge and concurrently degraded mobile genetic elements such as plasmids, thereby effectively blocking plasmid-mediated conjugative transfer of ARGs [33]. Additionally, this process promotes the release of intracellular ARGs from disrupted ARB hosts, leading to an increase in extracellular ARGs, which is consistent with our observations of inhibited conjugation and enhanced transformation. Another study employing a peroxymonosulfate / catalytic membrane-UV system similarly reports effective elimination of intracellular ARGs in bacteria from simulated aquaculture wastewater via ROS induction, achieving suppression of conjugation [34]. Wu *et al.* reveal that TiO_2 nanoparticle-mediated photocatalysis promotes filamentous phage f1 infection in bacteria collected from drinking water treatment plant samples, a trend that correlated with increased outer membrane permeability, F-pili-related gene expression, and pilus density—all attributed to oxidative stress [35]. Enhanced phage infection subsequently accelerates transduction-mediated ARG transfer, aligning with the findings of the present study. Furthermore, Xiao *et al.* confirm that TiO_2 photocatalysis facilitates phage transduction-mediated ARG transfer [17]. Notably, even in the presence of humic acid, a representative natural organic matter, TiO_2 photocatalysis still promotes phage-mediated ARG transduction [36]. Collectively, this body of evidence derived from photocatalytic disinfection studies conducted in real environmental water matrices supports the broader applicability of our conclusions.

In conclusion, this study demonstrated that photocatalytic water disinfection exerted significant and time- dependent effects on different HGT pathways. The initial enhancement of conjugative transfer and the sustained presence of transduction indicate that relying solely on bacterial inactivation to evaluate the effectiveness of this technology in reducing the spread of antibiotic resistance is limited. This study provides compelling evidence that the heterogeneous enhancement of resistance target structures, conferred by different ARGs, determines the preferred HGT pathway during photocatalytic disinfection. These findings emphasize that, when disinfecting wastewater or reclaimed water, it is essential to consider not only the inactivation of ARB but also the host-enhanced resistance targets associated with different ARGs. Such integrated consideration is critical for accurately predicting the environmental behavior and dissemination potential of ARGs.

3.3. Molecular regulatory mechanisms of different HGT modes

To clarify the molecular mechanisms driving the dynamic changes of HGT pathway, the expression of key functional genes involved in antibiotic resistance and HGT regulation during photocatalytic disinfection was further analyzed (Fig. 5). The results indicate that photocatalytic inactivation can inhibit bacterial cell function through multiple targets, systematically disrupting the molecular basis of HGT.

As shown in Fig. 5a, photocatalysis inactivation exhibited a broad-spectrum inhibitory effect on core genes associated with antibiotic resistance and essential cellular processes. During the initial 10 min photocatalytic process, cell membrane synthesis genes (*ompA* and *ompF*) of multiple *E. coli* strains resistant to CTX, PB, TET, SMZ, and NAL (*E. coli* DH5α (CTX), *E. coli* DH5α (PB), *E. coli* DH5α (TET), *E. coli* DH5α (SMZ), and *E. coli* DH5α (NAL)) were observed to be concurrently upregulated (Fig. 5a). This molecular regulation is consistent with the significant promotion of conjugation (Fig. 3a), suggesting that rapid remodeling of the bacterial membrane may contribute to the initial surge in plasmid transfer. This phenomenon can be attributed to the elevation of intracellular ROS levels at the early stage of photocatalytic treatment (Fig. S6a), which in turn increases membrane permeability (Fig. S7). Collectively, these results demonstrate that the ROS surge ultimately leads to the up-regulation of cell membrane synthesis genes (*ompA*, *ompF*). The initial stability of cell wall synthesis genes (*PBP2* and *PBP5*) and protein synthesis genes (*rsmB* and *rsmE*) suggests that maintaining an intact cellular structure is critical for facilitating early conjugation (Fig. 6). In contrast, the significant up-regulation of dihydrofolate synthetase genes (*folA* and *folP*) in RA-resistant *E. coli* (*E. coli* DH5α (RA)) was consistent with the suppressed phenomenon of conjugative transfer, indicating that these genes exert an antagonistic effect in the regulation of plasmid transfer. However, the aforementioned genes showed a significant rebound after 40 min inactivation across all resistant strains. This coordinated regulation elucidated the efficient inactivation of host bacteria (Figs. S3 and 2) and established the mechanistic foundation for the ultimate inhibition of conjugation. In detail, excessive ROS levels directly overwhelm the antioxidant defense system (Fig. S6), rendering it incapable of counteracting the potent oxidative stress. This overwhelming oxidative stress subsequently impairs cell membrane synthesis, thereby suppressing conjugation. The significant reduction of outer membrane protein genes (*ompA* and *ompF*) directly impairs membrane permeability and pili assembly function, which is consistent with the observed obstruction of intercellular contact and the eventual decline in conjugation frequency following the initial rebound (Figs. 3a and 4). Meanwhile, the marked down-regulation of β-lactamase gene ($bla_{CTX\text{-}M}$) confirms that photocatalytic inactivation directly targets and inhibits the expression of ARGs, thereby reducing the functional payload available for HGT. By coordinating the up-regulation of genes involved in DNA supercoiling (*gyrA*), folate metabolism (*folA* and *folP*), and membrane transport (*ompA* and *ompF*), the mechanical links associated with enhanced transformation were identified (Figs. 3b and S4b). This indicates that DNA replication, metabolic status, and membrane permeability exist in functional coordination during the regulation of transformation. In contrast, the dynamic expression of the RNA polymerase β subunit gene (*rpoB*), which trends in response to transduction frequency (Figs. 3c and S4c), suggests that it has a specific role in regulating the phage-mediated transduction pathway.

Furthermore, direct molecular insights into the pathway-specific regulation of HGT, as well as the expression of key regulatory genes for conjugation (*ftsY*, *korA*, and *tesB*), transformation (*lexA* and *umuD*), and transduction (*sspA* and *rpoS*) are presented in Fig. 5b. The initial up-regulation of the conjugation regulators *ftsY* and *tesB* was precisely correlated with the hormetic promotion of conjugation frequency observed during the same early-treatment phase (Figs. 3a and S4a), whereas *korA* showed an opposite trend. This suggests that sub-lethal photocatalytic inactivation temporarily activates plasmid-borne regulatory systems, thereby facilitating conjugative transfer. However, with prolonged treatment, the expression of *ftsY* and *tesB* was suppressed, which coincides with the eventual collapse of conjugation. This trend can be attributed to the excessive elevation of intracellular ROS levels (Fig. S6a), coupled with the incapacity of the antioxidant defense system to counteract this oxidative burst (Fig. S6b), ultimately disrupting the cellular redox balance. The regulatory network of conjugation involves the critical balance of positive and negative factors. Although the initial up-regulation of *ftsY* and *tesB* promotes conjugation by enhancing cell membrane contact [37,38], this process is eventually inhibited by the

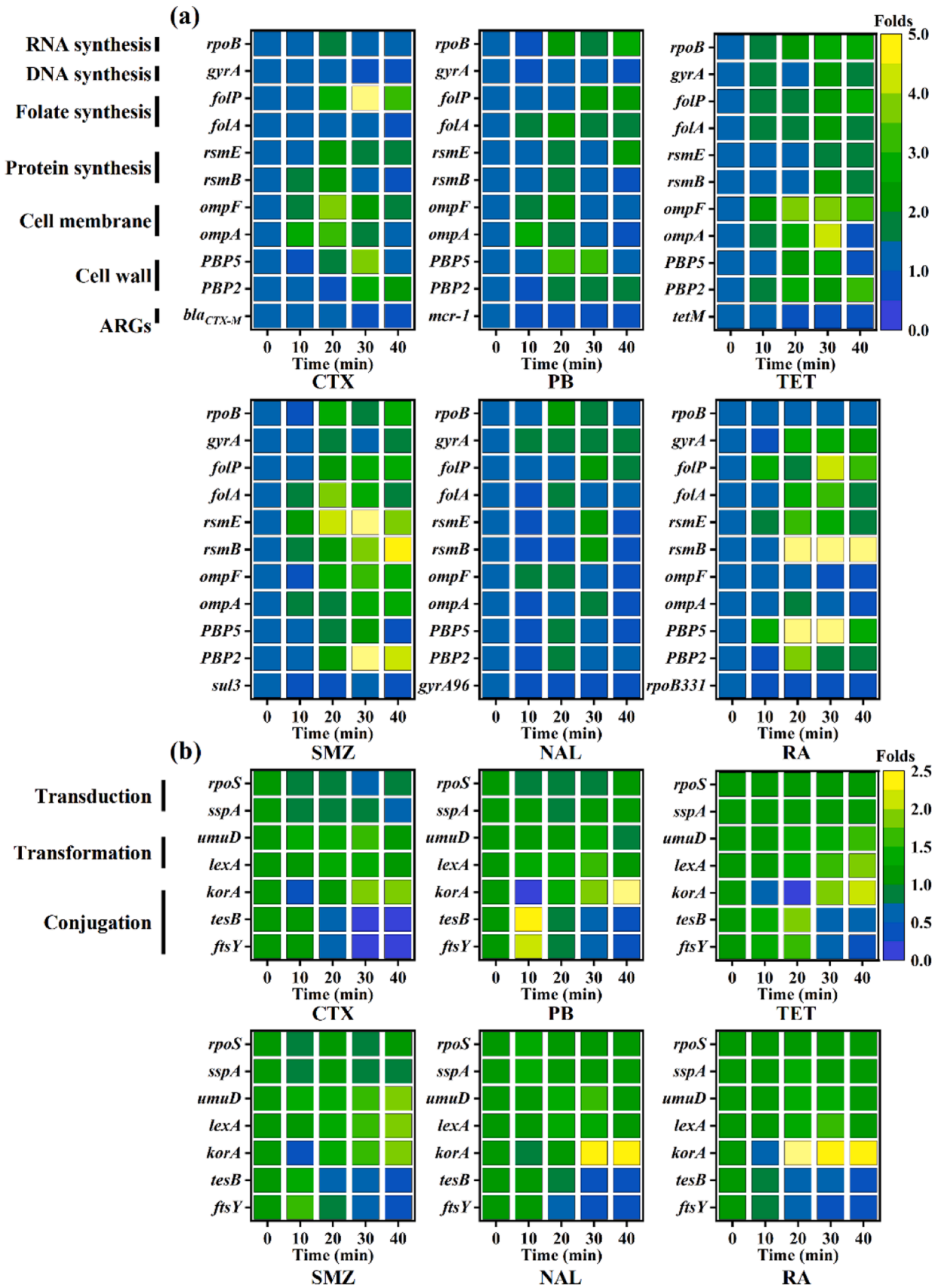

Fig. 5. Expression profiles of (a) antibiotic resistance genes and different resistance targets, and (b) key regulatory genes associated with conjugation, transformation, and transduction. CTX: *E. coli* DH5α (CTX); PB: *E. coli* DH5α (PB); TET: *E. coli* DH5α (TET); SMZ: *E. coli* DH5α (SMZ); NAL: *E. coli* DH5α (NAL); RA: *E. coli* DH5α (RA).

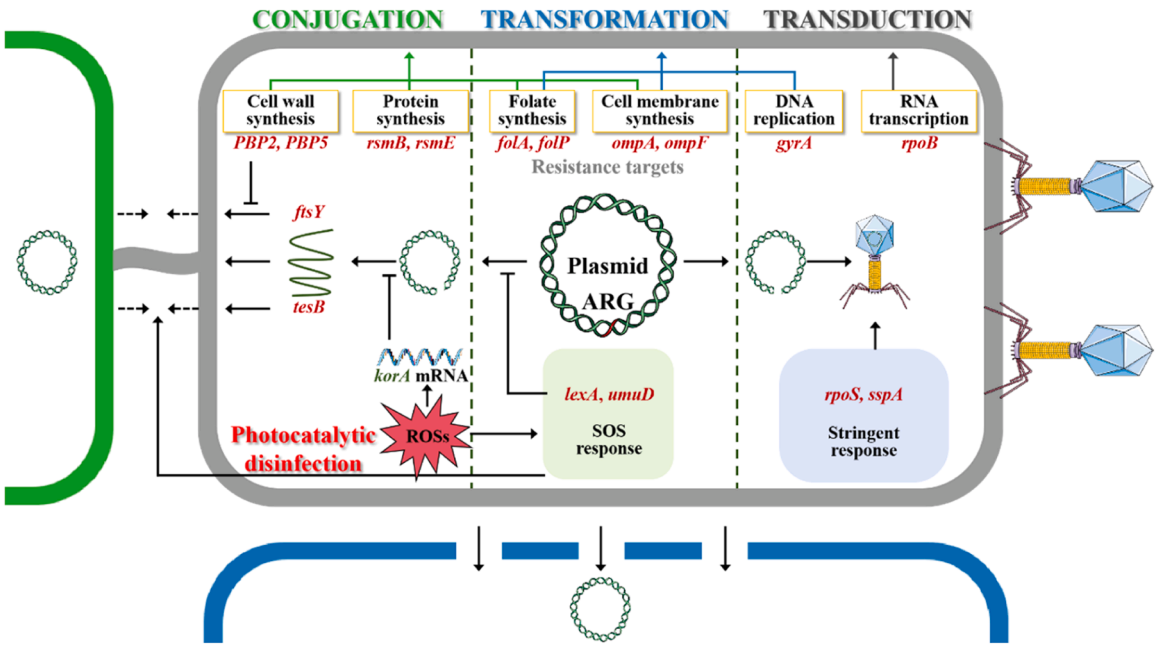

Fig. 6. Proposed molecular regulatory mechanisms underlying conjugation, transformation, and transduction during photocatalytic disinfection.

late up-regulation of penicillin-binding proteins (*PBP2* and *PBP5*), which inhibit the activity of FtsY [39,40]. Meanwhile, the conjugative process was negatively regulated by *korA*, which hinders plasmid unwinding [41]. In summary, these regulatory genes collectively constituted a multi-tiered control system for HGT pathways (Fig. 6). During the transformation process, the SOS response genes *lexA* and *umuD* exhibited persistent up-regulation. This is consistent with the sustained or even enhanced transformation frequency and transformant density observed in Figs. 3b and S4b, indicating that the bacterial SOS response and transformation are activated by DNA damage induced by photocatalysis inactivation. In detail, photocatalytic disinfection triggered the generation of intracellular ROS within bacteria (Fig. S6a). The accumulation of ROS subsequently provokes the bacterial SOS response, a notion supported by the observed elevation in total antioxidant capacity (Fig. S6b). This, in turn, activated the SOS response, which protects ARGs in plasmid from damage and preserves their transformation function (Fig. 6). The SOS response is a conserved bacterial stress response that functions as a key regulatory factor in HGT. This view is supported by previous studies, which indicate that it not only promotes conjugative transfer but also protects ARGs during transformation to ensure their functionality [42–44]. Notably, regulatory genes associated with transduction, including the stringent response regulatory genes *sspA* and *rpoS,* as well as the SOS response genes *umuD* and *lexA*, all exhibited significant and sustained up-regulation during photocatalytic inactivation. This molecular response offers a convincing explanation for the significant resilience of transduction observed in Figs. 3c and S4c. The photocatalytic-induced stress triggers a robust SOS response, which may promote the induction of prophages and DNA packaging. Since the stringent response has been shown to be critical for ARG transduction [45,46], we proposed that photocatalytic disinfection simultaneously activates both the stringent and SOS responses. These connected stress response pathways collectively preserve the functionality and integrity of DNA, thus playing a central role in regulating the transduction of ARGs (Fig. 6). Furthermore, the inactivation of bacteria merely means that they have completely lost culturability, while intracellular enzymes, energy, and raw materials are still sufficient to support phage-mediated packaging of plasmids. Therefore, even when bacterial populations are inactivated, phage-mediated gene transfer remains persistently active, while the originally dominant conjugative transfer is suppressed, resulting in the observed dominance of transduction in the later stages of photocatalytic disinfection (Fig. 4). In real water matrices, multiple factors may influence transduction-mediated ARG dissemination, including the natural inactivation of phages, resistance of indigenous bacteria to phages, and efficiency of ARG-packaging into phage particles. Beyond the well-established P1 phage model for generalized transduction in *E. coli*, numerous studies have documented the transduction residual risk of environmental phages. For instance, Sabatino *et al.* compare the phage resistome and bacterial resistome in two wastewater treatment plants (WWTPs) using shotgun metagenomics and find that disinfection exerts only marginal effects on phage community composition [47]. Another study reports the persistence of infectious Shiga toxin-encoding phages in a mesocosm experiment following disinfection, with these phages retaining their lytic capacity against *E. coli*, whereas the inactivation rate of Shiga toxin-producing *E. coli* is substantially higher [48]. Collectively, these findings indicate that environmental phages are considerably more tolerant to various adverse stressors than their bacterial hosts. Furthermore, Xiao *et al.* demonstrate that TiO_2 photocatalysis promotes filamentous phage gM13-mediated transduction in its *E. coli* host, and filamentous phages are ubiquitous in all aquatic environments [17]. Silver nanoparticles have also been shown to facilitate filamentous prophage hM13-mediated transduction of ARGs in both planktonic bacteria and those attached to microplastics [49]. Li *et al.* characterize phage-associated ARGs in samples collected from nine WWTPs and observe an increase in mobile genetic elements associated with phage-related processes from influent to effluent (from 12.68% to 21.10%), suggesting that phage-mediated transduction exacerbates the persistence and dissemination of ARGs within WWTPs [50]. Moreover, diverse ARGs have been identified in the genomes of phages isolated from various environments, further supporting the ubiquity of transduction by environmental phages [51,52]. Collectively, this body of evidence substantially extends the applicability of the transduction residual risk concept to real-world environmental contexts.

In all, the molecular evidence presented in Fig. 5 shows that photocatalytic bacterial inactivation does not operate through a single mechanism, but rather involves a complex time-dependent regulation of gene expression. The initial transient activation of conjugation regulators is succeeded by comprehensive cellular dormancy, while the sustained activation of SOS response and stringent response contributes to the predominant shift toward transformation, ultimately rendering transduction the primary residual risk for the dissemination of ARG. This

gene-level analysis confirms that evaluating disinfection efficacy based solely on bacterial inactivation is inadequate. The molecular machinery for HGT, especially transduction, can remain active even in decaying cell populations, potentially promoting further transfer of bacterial antibiotic resistance.

4. Conclusions

This study systematically reveals the dynamic dissemination patterns of ARGs through different HGT pathways during photocatalytic water disinfection. Early-stage photocatalysis heterogeneously promotes conjugation, primarily due to the reinforcement of host resistance target structures conferred by different ARGs. This target-specific structural enhancement accounts for the varied conjugation responses observed among ARGs with distinct resistance targets. Prolonged photocatalytic treatment induces a fundamental shift in the dominant HGT pathway, with conjugation ultimately switching to transduction. This transition is mechanistically driven by sustained activation of the SOS and stringent responses, coupled with progressive membrane damage, which collectively suppress conjugation while maintaining transduction.

These findings carry important environmental implications. The persistence of transduction demonstrates that phages serve as stable vectors for ARGs sustaining HGT after disinfection. More critically, the heterogeneous enhancement of resistance targets by different ARGs dictates their preferential HGT pathways, underscoring the need to consider target-specific responses in risk assessment. Current disinfection assessments relying solely on bacterial inactivation are insufficient, and the heterogeneous enhancement of resistance targets by different ARGs and the transduction residual risk must be incorporated into risk evaluation frameworks. Methodologically, combining gene expression analysis with HGT frequency monitoring provides novel insights into the molecular regulatory networks governing ARG dissemination. Overall, this work enhances our understanding of ARG behavior during disinfection and supports the development of more effective strategies for controlling antibiotic resistance in water environments.

Environmental implications

This study reveals that photocatalytic disinfection, while effectively inactivating bacteria, fails to eliminate the risk of ARG dissemination due to the transduction-associated residual risk. The heterogeneous, resistance target-dependent promotion of conjugation during early disinfection, followed by a definitive shift from conjugation to transduction as the dominant HGT mode, underscores a critical oversight in current disinfection assessment that relies solely on bacterial inactivation. Therefore, integrating resistance target characteristics and HGT mode-specific responses into disinfection evaluation frameworks is essential for developing truly effective water treatment technologies to combat antibiotic resistance and safeguard public health.

CRediT authorship contribution statement

Yongjie Liu: Methodology, Data curation. **Guiying Li:** Writing – review & editing, Funding acquisition. **Yiwei Cai:** Writing – original draft, Methodology, Formal analysis. **Taicheng An:** Supervision, Conceptualization. **Huijun Zhao:** Methodology, Conceptualization. **Po Keung Wong:** Methodology, Conceptualization.

Declaration of Competing Interest

The authors declare that they have no known competing financial interests or personal relationships that could have appeared to influence the work reported in this paper.

Acknowledgements

The author would like to thank financial supports from National Natural Science Foundation of China (42330702, 42077333, and 42407291), and Introduction Innovative and Research Teams Project of Guangdong Pearl River Talents Program (2023ZT10L102).

Appendix A. Supporting information

Supplementary data associated with this article can be found in the online version at doi:10.1016/j.jhazmat.2026.142480.

Data availability

No data was used for the research described in the article.

References

[1] Macallister, D., 2024. John, Groundwater decline is global but not universal. Nature 625, 668–670.
[2] Liu, Y., Shan, X., Liu, C., Chen, H., 2025. Microcosm experiments deciphered resistome coalescence, risks and source-sink relationship of antibiotic resistance in the soil irrigated with reclaimed water. J Hazard Mater 488, 137398.
[3] Shen, S., He, Z., Zhao, S., Zhu, Z., Wang, X., Tian, Y., Han, Y., Hu, M., Lu, C., Li, A., 2025. Environmental high-risk efflux pumps mediate concurrent enhancement of resistance and virulence in reclaimed water from urban wastewater treatment plants. J Hazard Mater 493, 138236.
[4] Hogard, S., Pearce, R., Gonzalez, R., Yetka, K., Bott, C., 2023. Optimizing ozone disinfection in water reuse: Controlling bromate formation and enhancing trace organic contaminant oxidation. Environ Sci Technol 57, 18499–18508.
[5] Lin, Z.-J., Zhou, Z.-C., Shuai, X.-Y., Shan, X.-Y., Zhou, J.-Y., Chen, H., 2024. Deciphering multidrug-resistant plasmids in disinfection residual bacteria from a wastewater treatment plant. Environ Sci Technol 58, 6793–6803.
[6] McKinney, C.W., Pruden, A., 2012. Ultraviolet disinfection of antibiotic resistant bacteria and their antibiotic resistance genes in water and wastewater. Environ Sci Technol 46, 13393–13400.
[7] Ji, H., Cai, Y., Wang, Z., Li, G., An, T., 2022. Sub-lethal photocatalysis promotes horizontal transfer of antibiotic resistance genes by conjugation and transformability. Water Res 221, 118808.
[8] Na, G., Wang, C., Gao, H., Li, R., Jin, S., Zhang, W., Zong, H., 2019. The occurrence of sulfonamide and quinolone resistance genes at the Fildes Peninsula in Antarctica. Mar Pollut Bull 149, 110503.
[9] Tan, Q., Li, W., Zhang, J., Zhou, W., Chen, J., Li, Y., Ma, J., 2019. Presence, dissemination and removal of antibiotic resistant bacteria and antibiotic resistance genes in urban drinking water system: A review. Front Environ Sci Eng 13, 36.
[10] Chen, X., Yin, H., Li, G., Wang, W., Wong, P.K., Zhao, H., An, T., 2019. Antibiotic-resistance gene transfer in antibiotic-resistance bacteria under different light irradiation: Implications from oxidative stress and gene expression. Water Res 149, 282–291.
[11] Guo, M.-T., Yuan, Q.-B., Yang, J., 2013. Ultraviolet reduction of erythromycin and tetracycline resistant heterotrophic bacteria and their resistance genes in municipal wastewater. Chemosphere 93, 2864–2868.
[12] Maganha de Almeida Kumlien, A.C., Borrego, C.M., Balcazar, J.L., 2021. Antimicrobial resistance and bacteriophages: An overlooked intersection in water disinfection. Trends Microbiol 29, 517–527.
[13] Bai, C., Cai, Y., Sun, T., Li, G., Wang, W., Wong, P.K., An, T., 2024. Mechanism of antibiotic resistance spread during sub-lethal ozonation of antibiotic-resistant bacteria with different resistance targets. Water Res 259, 121837.
[14] Wang, J.L., Chen, X.Y., 2022. Removal of antibiotic resistance genes (ARGs) in various wastewater treatment processes: An overview. Crit Rev Environ Sci Technol 52, 571–630.
[15] Agathokleous, E., Liu, C.-J., Calabrese, E.J., 2023. Applications of the hormesis concept in soil and environmental health research. Soil Environ Health 1, 100003.
[16] Jin, M., Liu, L., Wang, D.N., Yang, D., Liu, W.L., Yin, J., Yang, Z.W., Wang, H.R., Qiu, Z.G., Shen, Z.Q., Shi, D.Y., Li, H.B., Guo, J.H., Li, J.W., 2020. Chlorine disinfection promotes the exchange of antibiotic resistance genes across bacterial genera by natural transformation. ISME J 14, 1847–1856.
[17] Xiao, X., Ma, X.L., Han, X., Wu, L.J., Liu, C., Yu, H.Q., 2021. TiO2 photoexcitation promoted horizontal transfer of resistance genes mediated by phage transduction. Sci Total Environ 760, 144040.
[18] Yin, H., Cai, Y., Li, G., Wang, W., Wong, P.K., An, T., 2022. Persistence and environmental geochemistry transformation of antibiotic-resistance bacteria/genes in water at the interface of natural minerals with light irradiation. Crit Rev Environ Sci Technol 52, 2270–2301.
[19] Yin, H., Chen, X., Li, G., Wang, W., Wong, P.K., An, T., 2021. Can photocatalytic technology facilitate conjugative transfer of ARGs in bacteria at the interface of natural sphalerite under different light irradiation? Appl Catal B Environ 287, 119977.
[20] Liu, Y., Cai, Y., Li, G., Wang, W., Wong, P.K., An, T., 2022. Response mechanisms of different antibiotic-resistant bacteria with different resistance action targets to the stress from photocatalytic oxidation. Water Res 218, 118407.

[21] Arnold, B.J., Huang, I.T., Hanage, W.P., 2021. Horizontal gene transfer and adaptive evolution in bacteria. Nat Rev Microbiol 20, 206–218.
[22] von Wintersdorff, C.J., Penders, J., van Niekerk, J.M., Mills, N.D., Majumder, S., van Alphen, L.B., Savelkoul, P.H., Wolffs, P.F., 2016. Dissemination of antimicrobial resistance in microbial ecosystems through horizontal gene transfer. Front Microbiol 7, 173.
[23] Domingues, S., Nielsen, K.M., 2017. Membrane vesicles and horizontal gene transfer in prokaryotes. Curr Opin Microbiol 38, 16–21.
[24] Imlay, J.A., 2013. The molecular mechanisms and physiological consequences of oxidative stress: lessons from a model bacterium. Nat Rev Microbiol 11, 443–454.
[25] Zhang, Y., Gu, A.Z., He, M., Li, D., Chen, J.M., 2017. Subinhibitory concentrations of disinfectants promote the horizontal transfer of multidrug resistance genes within and across genera. Environ Sci Technol 51, 570–580.
[26] Wang, Q., Mao, D.Q., Luo, Y., 2015. Ionic liquid facilitates the conjugative transfer of antibiotic resistance genes mediated by plasmid RP4. Environ Sci Technol 49, 8731–8740.
[27] Bru, J.-L., Rawson, B., Trinh, C., Whiteson, K., Hoyland-Kroghsbo, N.M., Siryaporn, A., 2019. PQS produced by the *Pseudomonas aeruginosa* stress response repels swarms away from bacteriophage and antibiotics. J Bacteriol 201, e00383-00319.
[28] Johnston, C., Martin, B., Fichant, G., Polard, P., Claverys, J.-P., 2014. Bacterial transformation: distribution, shared mechanisms and divergent control. Nat Rev Microbiol 12, 181–196.
[29] Hajipour, M.J., Fromm, K.M., Akbar Ashkarran, A., Jimenez de Aberasturi, D., Larramendi, I.Rd, Rojo, T., Serpooshan, V., Parak, W.J., Mahmoudi, M., 2012. Antibacterial properties of nanoparticles. Trends Biotechnol 30, 499–511.
[30] Botelho, J., Schulenburg, H., 2021. The role of integrative and conjugative elements in antibiotic resistance evolution. Trends Microbiol 29, 8–18.
[31] Li, B., Qiu, Y., Song, Y., Lin, H., Yin, H., 2019. Dissecting horizontal and vertical gene transfer of antibiotic resistance plasmid in bacterial community using microfluidics. Environ Int 131, 105007.
[32] Haudiquet, M., Buffet, A., Rendueles, O., Rocha, E.P.C., 2021. Interplay between the cell envelope and mobile genetic elements shapes gene flow in populations of the nosocomial pathogen *Klebsiella pneumoniae*. PLoS Biol 19, e3001276.
[33] Yu, H., Zhang, X., Zhao, J., Sun, T., Zhu, Y., 2025. Mechanism of TiO2 nanotube UV-photocatalytic degradation of antibiotic resistance genes in the wastewater sludge and blocking of the transfer. Front Environ Sci 13, 1590101.
[34] Hou, X., Zhang, Y., Wang, M., Lu, J., Ma, D., Li, Q., Li, L., Wang, Z., Gao, B., Wang, Y., 2024. Synergistic singlet oxygen and UV irradiation for efficient intracellular ARGs removal via peroxymonosulfate/catalytic membrane-UV system. J Hazard Mater 480, 136385.
[35] Wu, S., Huttelmaier, S., Sumner, J., Hartmann, E., Gray, K., 2026. Sublethal effects of photoactive engineered nanomaterials on filamentous bacteriophage infection and *E. coli* gene expression in freshwater. Environ Sci Nano 13, 478–495.
[36] Zhang, Q.R., Zhou, H.X., Qiao, J., Jiang, P., Xiao, X., 2024. New insight into nanomaterial-mediated dissemination of phage-borne resistance genes: Roles of humic acid and illumination. Chem Eng J 486, 150276.
[37] de Leeuw, E., Kaat, K.T., Moser, C., Menestrina, G., Demel, R., de Kruijff, B., Oudega, B., Luirink, J., Sinning, I., 2000. Anionic phospholipids are involved in membrane association of FtsY and stimulate its GTPase activity. EMBO J 19, 531–541.
[38] Derewenda, Z.S., Li, J., Derewenda, U., Dauter, Z., Smith, S., 2000. Crystal structure of the *Escherichia coli* thioesterase II, a homolog of the human Nef binding enzyme. Nat Struct Biol 7, 555–559.
[39] Braig, D., Bär, C., Thumfart, J.-O., Koch, H.-G., 2009. Two cooperating helices constitute the lipid-binding domain of the bacterial SRP receptor. J Mol Biol 390, 401–413.
[40] Ferreira, L.C., Keck, W., Betzner, A., Schwarz, U., 1987. vivo cell division gene product interactions in *Escherichia coli* K-12. J Bacteriol 169, 5776–5781.
[41] Qiu, Z., Yu, Y., Chen, Z., Jin, M., Yang, D., Zhao, Z., Wang, J., Shen, Z., Wang, X., Qian, D., Huang, A., Zhang, B., Li, J.-W., 2012. Nanoalumina promotes the horizontal transfer of multiresistance genes mediated by plasmids across genera. Proc Natl Acad Sci USA 109, 4944–4949.
[42] Janion, C., 2008. Inducible SOS response system of DNA repair and mutagenesis in *Escherichia coli*. Int J Biol Sci 4, 338–344.
[43] Rajagopalan, M., Lu, C., Woodgate, R., O'Donnell, M., Goodman, M.F., Echols, H., 1992. Activity of the purified mutagenesis proteins UmuC, UmuD', and RecA in replicative bypass of an abasic DNA lesion by DNA polymerase III. Proc Natl Acad Sci USA 89, 10777–10781.
[44] Beaber, J.W., Hochhut, B., Waldor, M.K., 2004. SOS response promotes horizontal dissemination of antibiotic resistance genes. Nature 427, 72–74.
[45] Li, L., Rao, N.N., Kornberg, A., 2007. Inorganic polyphosphate essential for lytic growth of phages P1 and fd. Proc Natl Acad Sci USA 104, 1794–1799.
[46] Sass, T.H., Lovett, S.T., 2024. The DNA damage response of *Escherichia coli*, revisited: Differential gene expression after replication inhibition. Proc Natl Acad Sci USA 121, e2407832121.
[47] Sabatino, R., Sbaffi, T., Sivalingam, P., Corno, G., Fontaneto, D., Di Cesare, A., 2023. Bacteriophages limitedly contribute to the antimicrobial resistome of microbial communities in wastewater treatment plants. Microbiol Spectr 11, e0110123.
[48] Allué-Guardia, A., Martínez-Castillo, A., Muniesa, M., Elkins, C.A., 2014. Persistence of infectious shiga toxin-encoding bacteriophages after disinfection treatments. Appl Environ Microbiol 80, 2142–2149.
[49] Zhang, Q., Zhou, H., Jiang, P., Wu, L., Xiao, X., 2024. Silver nanoparticles facilitate phage-borne resistance gene transfer in planktonic and microplastic-attached bacteria. J Hazard Mater 469, 133942.
[50] Li, Z., Guo, X., Liu, B., Huang, T., Liu, R., Liu, X., 2024. Metagenome sequencing reveals shifts in phage-associated antibiotic resistance genes from influent to effluent in wastewater treatment plants. Water Res 253, 121289.
[51] Debroas, D., Siguret, C., 2019. Viruses as key reservoirs of antibiotic resistance genes in the environment. ISME J 13, 2856–2867.
[52] Cao, H., Liu, S., Cai, P., Li, P., Wang, J., Ni, J., 2026. Phage-mediated resistome dynamics in global aquifers. Nat Water 4, 78–90.